Journal of Experimental Botany, Vol. 70, No. 15 pp. 3795–3808, 2019
doi:10.1093/jxb/erz193 Advance Access Publication 25 April, 2019
This paper is available online free of all access charges (see https://academic.oup.com/jxb/pages/openaccess for further details)

RESEARCH PAPER

Maize pentatricopeptide repeat protein DEK41 affects *cis*-splicing of mitochondrial *nad4* intron 3 and is required for normal seed development

Chenguang Zhu[1,†], Guangpu Jin[1,†], Peng Fang[1], Yan Zhang[1], Xuzhen Feng[1], Yuanping Tang[1], Weiwei Qi[1] and Rentao Song[1,2,*],

[1] Shanghai Key Laboratory of Bio-Energy Crops, Plant Science Center, School of Life Sciences, Shanghai University, Shanghai 200444, China
[2] State Key Laboratory of Plant Physiology and Biochemistry, National Maize Improvement Center, Beijing Key Laboratory of Crop Genetic Improvement, Joint International Research Laboratory of Crop Molecular Breeding, College of Agronomy and Biotechnology, China Agricultural University, Beijing 100193, China

[†] These authors contributed equally to this work.
* Correspondence: rentaosong@cau.edu.cn

Received 31 December 2018; Editorial decision 10 April 2019; Accepted 10 April 2019

Editor: Karl-Josef Dietz, Bielefeld University, Germany

Abstract

The splicing of organelle-encoded mRNA in plants requires proteins encoded in the nucleus. The mechanism of splicing and the factors involved are not well understood. Pentatricopeptide repeat (PPR) proteins are known to participate in such RNA–protein interactions. Maize *defective kernel 41* (*dek41*) is a seedling-lethal mutant that causes developmental defects. In this study, the *Dek41* gene was cloned by *Mutator* tag isolation and allelic confirmation, and was found to encode a P-type PPR protein that targets mitochondria. Analysis of the mitochondrial RNA transcript profile revealed that *dek41* mutations cause reduced splicing efficiency of mitochondrial *nad4* intron 3. Immature *dek41* kernels exhibited severe reductions in complex I assembly and NADH dehydrogenase activity. Up-regulated expression of alternative oxidase genes and deformed inner cristae of mitochondria in *dek41*, as revealed by TEM, indicated that proper splicing of *nad4* is essential for correct mitochondrial functioning and morphology. Consistent with this finding, differentially expressed genes in the *dek41* endosperm included those related to mitochondrial function and activity. Our results indicate that DEK41 is a PPR protein that affects *cis*-splicing of mitochondrial *nad4* intron 3 and is required for correct mitochondrial functioning and maize kernel development.

Keywords: *dek41*, mitochondria, *nad4*, pentatricopeptide repeat protein, RNA splicing, *Zea mays*.

Introduction

Maize (*Zea mays*) is widely used for genetic research due to its easily observable phenotypes, and the broad range of *defective kernel* (*dek*) mutants provide good tools for investigating kernel development (Neuffer and Sheridan, 1980). Many maize *dek* mutants have been identified, for example *dek1* exhibits severe growth and development defects (Lid *et al.*, 2002), *reas1* causes a mild developmental delay (Qi *et al.*, 2016), and mutants of pentatricopeptide repeat (PPR) proteins exhibit reduced kernel size and arrested development of the embryo and endosperm (Liu *et al.*, 2013; Sun *et al.*, 2015; Cai *et al.*, 2017; Dai *et al.*, 2018). Thus, *dek* mutants offer opportunities to investigate many basic biological processes during kernel development.

In higher plants, the nucleus-encoded PPR proteins primarily localize to chloroplasts and mitochondria, and play critical roles in RNA editing, *cis*- and *trans*-splicing, cleavage, and maturation (Barkan and Small, 2014). PPR proteins are defined by tandem repeats of a degenerate 35-amino-acid motif and are classified into two major subgroups: P-type members possess only tandem repeats of the 35-amino-acid PPR motif, whilst PLS-type members include sequential repeats of P, short (S), and long (L) PPR motifs that often carry an E or E–DYW domain extension at the C terminus (Lurin *et al.*, 2004; Cheng *et al.*, 2016). In plants, the PPR family comprises more than 450 members, and a number of mutants associated with severe growth and development defects have been characterized (Fujii and Small, 2011; Barkan and Small, 2014; Hammani and Giegé, 2014; Møller, 2016; Gorchs Rovira and Smith, 2019). However, the regulatory functions of many PPR proteins have not yet been characterized.

Many P-type PPR proteins function in RNA processes including stabilization, cleavage, translational activation, and splicing. RNA splicing in mitochondria requires the coordination of PPR proteins because of the loss of the ability to self-splice (Bonen, 2008; Brown *et al.*, 2014). Group I and group II introns have distinct splicing patterns. More than 20 group II introns have been identified in the mitochondrial genomes of flowering plants, including 15 *cis*-spliced introns in *nad1*, *nad2*, *nad4*, *nad5*, *nad7*, *rps3*, *cox2*, and *ccmF*$_C$, and seven *trans*-spliced introns in *nad1*, *nad2*, and *nad5* (Burger *et al.*, 2003; Berrisford and Sazanov, 2009). In the mitochondrial genome, most introns are in genes that encode subunits of complex I (NADH dehydrogenase), which is located in the inner membrane and transfers electrons from NADH to the primary acceptor FMN followed by the ubiquinone-binding site (Sazanov and Hinchliffe, 2006; Berrisford and Sazanov, 2009). Five P-type PPR proteins are required for group II intron splicing of mitochondrial transcripts in Arabidopsis, including transcripts of *nad1* (de Longevialle *et al.*, 2007), *nad2* (Liu *et al.*, 2010), *nad5* (Colas des Francs-Small *et al.*, 2014), and *nad7* (Hsieh *et al.*, 2015). In maize, EMP10, EMP16, and DEK37 are involved in *cis*-splicing of *nad2* intron 4 and intron 1 (Xiu *et al.*, 2016; Cai *et al.*, 2017; Dai *et al.*, 2018), DEK2 is required for the *trans*-splicing of *nad1* intron 1 (Qi *et al.*, 2017b), and DEK35 affects *cis*-splicing of *nad4* intron 1 (Chen *et al.*, 2017). Studies of maize kernel mutants provide an opportunity to reveal the important roles of other P-type PPR proteins in *cis*- and *trans*-splicing of mitochondrial RNA.

Among the large family of PPR proteins in flowering plants, only a small subset has been studied at the molecular level, particularly for mitochondrial PPRs, in which mutations are frequently embryo-lethal. Determining the molecular functions of mitochondrial PPR proteins may shed light on RNA-processing mechanisms as well as on the assembly of the oxidative phosphorylation machinery. In the present study, a maize seed mutant *dek41* corresponding to a defective and seedling-lethal phenotype was characterized. *Dek41* encodes a P-type PPR protein that targets to the mitochondria. The *dek41* mutant shows reduced splicing efficiency of mitochondrial *nad4* intron 3 in developing seeds. Lack of this splicing process affects the accumulation of complex I and the activity of NADH dehydrogenase, leading to the arrest of mitochondrial functioning and kernel development.

Materials and methods

Plant materials

The *Zea mays MuDR* stock (330I) and UFMu01110 mutant line were obtained from Maize Genetics Cooperation Stock Center (http://maizecoop.cropsci.uiuc.edu). The *MuDR* stock was crossed into the B73 inbred line as the male parent to generate F1 population seeds, and then self-crossed to generate F2 population ears. Phenotypical screening for seed mutants was carried out on these F2 ears, which resulted in a new *dek* mutant being identified, and we designated it as *dek41-ref*. The *dek41-ref* mutant seeds on the F2 ear were white and during their development they were smaller than the wild-type (WT) seeds. The F2 ears of *dek41-ref* displayed a 1:3 segregation of mutant and WT seeds.

Mature seeds were used for genomic DNA extraction. Immature seeds were sampled for RNA and protein extraction, mitochondria isolation, preparation of paraffin and resin sections, TEM, and RNA-seq. Other plant tissues were harvested from one inbred B73 plant for RNA and protein extraction. All plants were cultivated in an experimental field in Shanghai University, Shanghai, China.

Measurement of protein and starch levels

For protein measurements, endosperms of mature WT and *dek41*-ref seeds were separated from the embryo and pericarp by dissection after soaking the seeds in water. The samples were dried to constant weight, ground with a mortar and pestle in liquid nitrogen. Proteins were extracted from 50 mg of three pooled endosperm powder samples from same ear, and then the protein content was measured according to a previously described protocol (Qi *et al.*, 2016). All the measurements were conducted on three biological replicates. For the starch measurements, mature seeds of the WT and *dek41* mutants were ground in liquid nitrogen and the resulting powders were dried to a constant weight. 100 mg of three pooled powders from same ear were used for the total starch measurements using an amyloglucosidase/α-amylase starch assay kit (Megazyme) according to a previously described protocol (Qi *et al.*, 2016). All the measurements were conducted on three biological replicates.

Light microscopy and TEM

For light microscopy, immature WT and *dek41*-ref seeds at 12 d after pollination (DAP), 15 DAP, and 18 DAP were collected from the same ear and were cut along the longitudinal axis for preparation of paraffin sections. The sections were fixed in a formalin–acetic acid–alcohol mixture and were dehydrated in an ethanol gradient series of 50, 60, 70, 85, 95, and 100%. After replacement of acetone and infiltration with paraffin, the sections were embedded and cut using a RM2265 microtome (Leica). The sections were stained with Basic Fuchsin Dye and were observed using a Leica DFC500 digital camera system.

For TEM analysis, immature WT and *dek41*-ref seeds at 15 DAP were collected from the same ear and were cut along the horizontal axis into small pieces and fixed in paraformaldehyde. The samples were further processed and stained by osmic acid, and were observed by TEM (Tecnai G^2 Spirit BioTWIN, FEI Company).

Mutator tag isolation

The *Mutator* tag isolation was performed according to Williams-Carrier *et al.* (2010), with some modifications. Genomic DNA was prepared for mechanical shearing by the Majorbio Bio-Pharm Technology Company, Ltd (Shanghai, China). Fragments (200–500 bp) were ligated to modified Illumina adapters to mark samples from different individuals. *Mu*-containing DNA fragments were enriched by hybridization to a biotinylated oligonucleotide corresponding to the end of the *Mu* terminal inverted repeat. Two successive hybrid enrichment steps were performed to ensure that most of the sequenced DNA fragments harbored *Mu* sequences. Using primers that bind to the ends of the adapters, 15 and 18 cycles of PCR were used to bulk-up the recovered DNA after the first and second selection rounds, respectively. The PCR products were cloned into the vector pMD18-T (Takara). The effectiveness of the enrichment

was tested by calculating the percentage of clones containing the *Mu* fragment. Enrichment rates above 30% were selected for *Mu* Illumina sequencing, which was carried out at BerryGenomics (Beijing, China).

RNA extraction and quantitative RT-PCR

Total RNA was extracted from the samples using TRIzol reagent (Tiangen) according to previous Feng *et al.* (2009), and DNA was removed by treatment with RNase-Free DNase I (Takara). Using ReverTra Ace reverse transcriptase (Toyobo), RNA was reverse-transcribed to complementary DNA using the random primers provided in the kit (ReverTra Ace qPCR RT Master Mix, Toyobo). Amplification of mitochondrial transcripts was performed using primers as described previously (Chen *et al.*, 2017). Quantitative RT-PCR was performed using three independent sets of RNA with *Ubiquitin* as the reference gene. Primers for the mitochondrial introns were designed as described previously with some modifications (Qi *et al.*, 2017b) (Supplementary Table S2 at *JXB* online). Quantitative RT-PCR was performed with SYBR Green Real-Time PCR Master Mix (Toyobo) using a Mastercycler ep realplex 2 (Eppendorf) according to the manufacturer's protocol.

Phylogenetic analysis of DEK41 and its homologs

Sequences were compared with NCBI GenBank entries (http://www.ncbi.nlm.nih.gov/) using the protein–protein BLAST. To align the sequences of DEK41 and its homologs, the software Clustal X 1.81 was used (Thompson *et al.*, 1997). A phylogenetic tree was constructed using the neighbour-joining method of the MEGA 4.0 program (Tamura *et al.*, 2007) with the bootstrap test based on 2000 replicates.

Subcellular localization of DEK41

The full-length DEK41 coding region was cloned into pENTR/D-TOPO (Invitrogen), and transferred into the binary vector pB7WGY2 to produce the *DEK41::EYFP* fusion construct through LR site-specific recombination. The *DEK41::EYFP* fusion was placed under a Cauliflower mosaic virus 35S promoter. The construct was introduced into *Agrobacterium tumefaciens* strain Gv3101 and infiltrated into *Nicotiana tabacum* leaf epidermal cells, as described by van Herpen *et al.* (2010). The fluorescence signals were detected by laser-scanning confocal microscopy using a Zeiss LSM710 30 h after infiltration. The mCherry marker pBIN20-MT-RK (Nelson *et al.*, 2007) was a commercial vector purchased from The Arabidopsis Information Resource (TAIR, https://www.arabidopsis.org). This vector was transferred into *Agrobacterium*, and the fluorescent signal observed after infecting tobacco mesophyll cells was used as a marker signal for mitochondria.

Preparation of mitochondria

Mitochondria were extracted from immature seeds of inbred B73 at 18 DAP as described previously (Chen *et al.*, 2017), with some modifications. Approximately 15 g of immature seeds was harvested from an individual plant at 18 DAP and ground into powder in liquid nitrogen with a mortar and pestle. Then, 20 ml of precooled (4 °C) extraction buffer (100 mM tricine, 300 mM sucrose, 10 mM KCl, 1 mM $MgCl_2$, 1 mM EDTA-K, 0.1% BSA, 5 mM DTT, pH 7.4) and 60 µl of plant protease inhibitor cocktail (Sigma-Aldrich) were added to the ground tissue. All the subsequent steps were performed at 4 °C. After filtration through a Miracloth membrane (Calbiochem, San Diego, CA), the samples were centrifuged twice at 2600 *g* for 15 min, and the supernatant was then centrifuged at 12 000 *g* for 25 min to pellet the crude mitochondria. The pellet was resuspended in wash buffer (100 mM tricine, 300 mM sucrose, 10 mM KCl, 1 mM $MgCl_2$, 1 mM EDTA-K, 0.1% BSA, pH 7.4) and loaded onto sucrose density gradients of 1.5, 2.5, 2.5, 2, and 2 ml respectively containing 1.8, 1.45, 1.2, 0.9, and 0.6 M sucrose diluted in wash buffer, as previously described (Clayton and Shadel, 2014). After 90 min of centrifugation at 62 000 *g* at 4 °C, the mitochondria were collected from the 1.2 M/1.45 M interface and washed four times in wash buffer. The purified mitochondria were collected after 20 min of centrifugation at 16 800 *g* at 4 °C.

BN-PAGE and NADH dehydrogenase activity

The isolated mitochondria were resuspended in 50 µl B25G20 solution (25 mM Bis-Tris, 20% glycerin, pH 7.0), with 20% *n*-Dodecyl β-D-maltoside (DDM) added to a final concentration of 1%, and were gently mixed on ice for 1.5 h. After 15 min of centrifugation at 15 800 *g* at 4 °C, the supernatant was collected and added to the loading buffer for blue native polyacrylamide electrophoresis (BN-PAGE). The concentration of the separation gel was from 5–13.5%. The electrophoresis was initially run at 50 V, and increased by 25 V every 20 min to a final level of 150 V until the loading dye migrated to the edge of the gel. The gel was stained with Coomassie brilliant blue. Measurement of NADH dehydrogenase activity was performed as described previously (Meyer *et al.* 2009). Briefly, the gel was washed three times for 5 min with distilled water and incubated in the reaction solution (0.14 mM NADH, 1.22 mM NBT, 0.1M Tris-HCl, pH 7.4). When the dark blue stain was strong enough, the reaction was stopped by transferring the gel to 40% (v/v) methanol /10% (v/v) acetic acid.

Immunoblot analysis

Total proteins were extracted from immature seeds of the WT and *dek41* mutants at 18 DAP, and were then separated by SDS-PAGE. Separated protein samples were transferred to a nitrocellulose membrane (0.45 µm; Millipore). The membrane with the protein sample attached was incubated with primary and secondary antibodies. The signal was visualized using a SuperSignal West Pico Chemiluminescent Substrate kit (Pierce) according to the manufacturer's instructions. To produce polyclonal antibodies against NAD4, the 55–71 amino acid sequence (PRIQFDPSTANSQFVESC) of NAD4 was synthesized. This peptide was synthesized and dissolved in PBS solution (1.37M NaCl, 0.1M Na_2HPO_4, 0.018M KH_2PO_4, KCl 0.027M) containing 8 M urea, and was then coupled to KLH (keyhole limpet hemocyanin) protein for immunization in rabbits by the Shanghai Ying Ji Biotechnology Co., Ltd, according to standard protocols. The polyclonal antibodies against NAD4 were used at a dilution of 1:1000. The antibodies raised for NAD4 recognized a protein of an apparent molecular weight of 70 kDa (see Supplementary Fig. S1). Antibodies against cytochrome c (Agrisera) and α-tubulin (Sigma-Aldrich) were used at a dilution of 1:5000.

RNA-seq analysis

Total RNA was extracted from developing WT and *dek41*-ref seeds at 12 DAP. Library construction was performed according to Illumina standard protocols. Reads were aligned to the maize B73 genome using Bowtie 2 v2.1.0 (Langmead and Salzberg, 2012). Data were normalized as reads per kilobase of exon model per million mapped reads (RPKM), as the sensitivity of RNA-seq depends on both molar concentration and transcript length (Mortazavi *et al.*, 2008). Significant differentially expressed genes (DEGs) were identified as those with a fold-change >2.0 and $P<0.001$.

Data availability

The RNA-seq data are available from the NCBI Gene Expression Omnibus (http://www.ncbi.nlm.nih.gov/geo) under the series entry GSE117091. Sequence data from this paper can be found in the GenBank/EMBL data libraries under the following accession numbers: DEK41, ONM56221, GRMZM2G127015; NAD4, AAR91196.

Results

dek41 *mutants display defective seed development*

dek41 is a *defective kernel* (*dek*) mutant that was isolated from F2 populations containing active *MuDR* (see Methods). F2 ears that displayed a 3:1 segregation (589:207, from three ears, $P<0.05$) of WT to *dek* phenotypes were termed *dek41*-ref. The *dek41*-ref mutant had white seeds that were smaller than

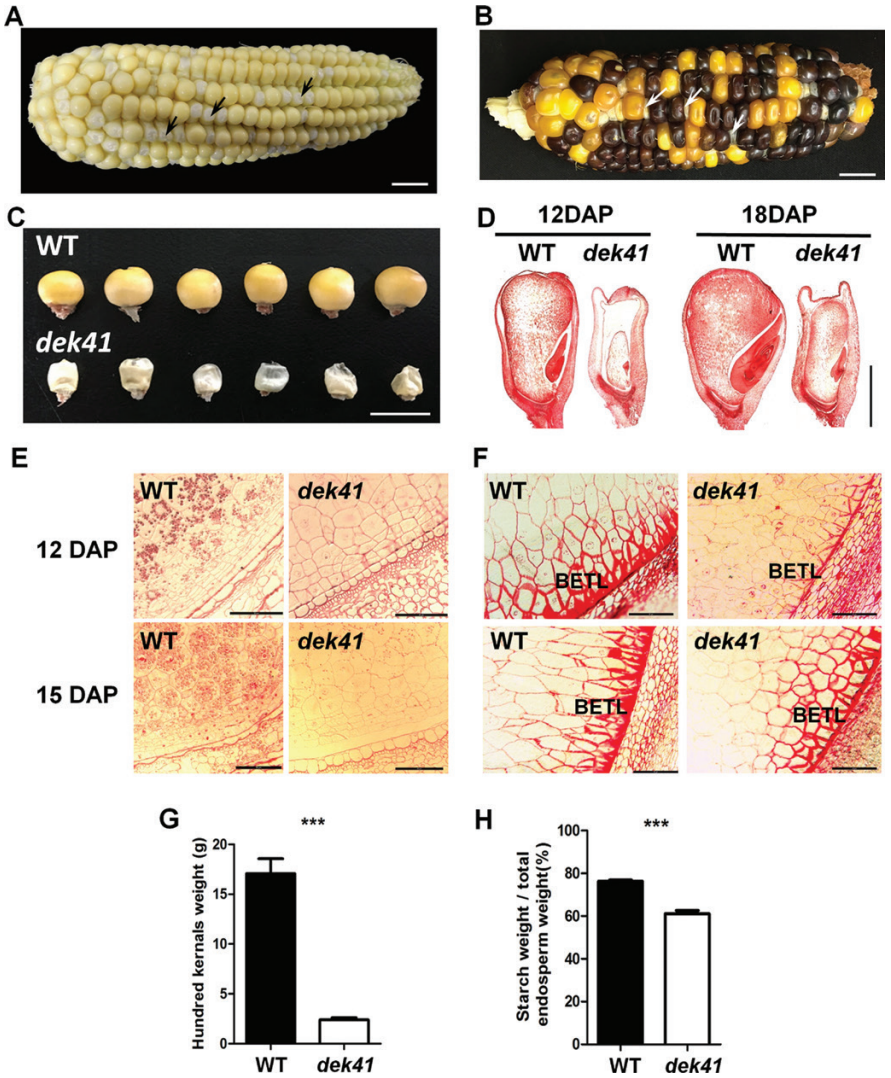

Fig. 1. Phenotypic features of the maize *dek41* mutant. (A) Ear of an F2 plant of *dek41*/wild-type (WT) at 12 d after pollination (DAP). The arrows indicate examples of mutant seeds. Scale bar is 1 cm. (B) A mature F2 ear of *dek41*/WT. The arrows indicate examples of mutant seeds. Scale bar is 1 cm. (C) Examples of mature WT and *dek41* seeds from the segregated F2 population. Scale bar is 1 cm. (D) Paraffin sections of WT and *dek41* seeds at 12 DAP and 18 DAP. Scale bar is1.5 mm. (E) Microstructure of developing endosperms of WT and *dek41* at 12 DAP and 15 DAP. Scale bars are 100 μm. (F) Paraffin sections of the basal endosperm transfer layer of WT and *dek41* at 12 DAP and 15 DAP. Scale bars are 50 μm. (G) Comparison of 100-seed weight of randomly selected mature WT and *dek41* seeds in the segregated F2 population. Data means (±SE) of n=3 individual plants. (H) Comparison of total starch content in mature WT and *dek41* endosperm, expressed as percentage dry weight. Data are means (±SE) of n=3 individual plants. Significant differences in (G, H) were determined using Student's t-test: $^{***}P<0.001$. (This figure is available in colour at *JXB* online.)

WT during seed development (12 DAP) (Fig. 1A). Mature homozygous kernels of the *dek41* mutants were small and flat, and had empty pericarps at the top of kernels (Fig. 1B, C). The 100-kernel weight of mutant seeds was only 13% that of the WT (Fig. 1G) and the total percentage starch content by weight was reduced by 20% (Fig. 1H). The zein protein and total protein contents of mature endosperm were also lower in mutant kernels than in the WT (Supplementary Fig. S2).

Detailed phenotypic examination of WT and *dek41*-ref seeds at different developmental stages showed that embryo and endosperm development in the *dek41*-ref mutant was delayed at least 6 d compared to the WT (Fig. 1D). The endosperm cells of seeds of the *dek41* mutants at 12 DAP and 15 DAP were less cytoplasmically dense with fewer starch granules compared to the WT (Fig. 1E). Analysis of paraffin sections at 12 DAP and 15 DAP showed that the development of the basal endosperm transfer layer was arrested in *dek41* kernels (Fig. 1F). The *dek41* seeds showed very low germination rates, and no seedlings survived after germination. Together, these results indicated that the growth and development of *dek41* seeds were severely affected and that the homozygous *dek41* mutation was seedling-lethal.

Cloning of Dek41

We used F2 seeds of *dek41*-ref exhibiting a 3:1 segregation ratio (589:207, $P<0.05$) for genetic mapping. After characterizing 170 individual seeds, *Dek41* was mapped between the markers InDel-6 and InDel-7, a region at ~9 Mb on chromosome 7 (maize B73 RefGen_v3) (Fig. 2A). As *dek41*-ref was isolated from an active *Mutator* line, *Mu* tags were isolated and sequenced (Williams-Carrier *et al.*, 2010). Only one unique *Mu* insertion

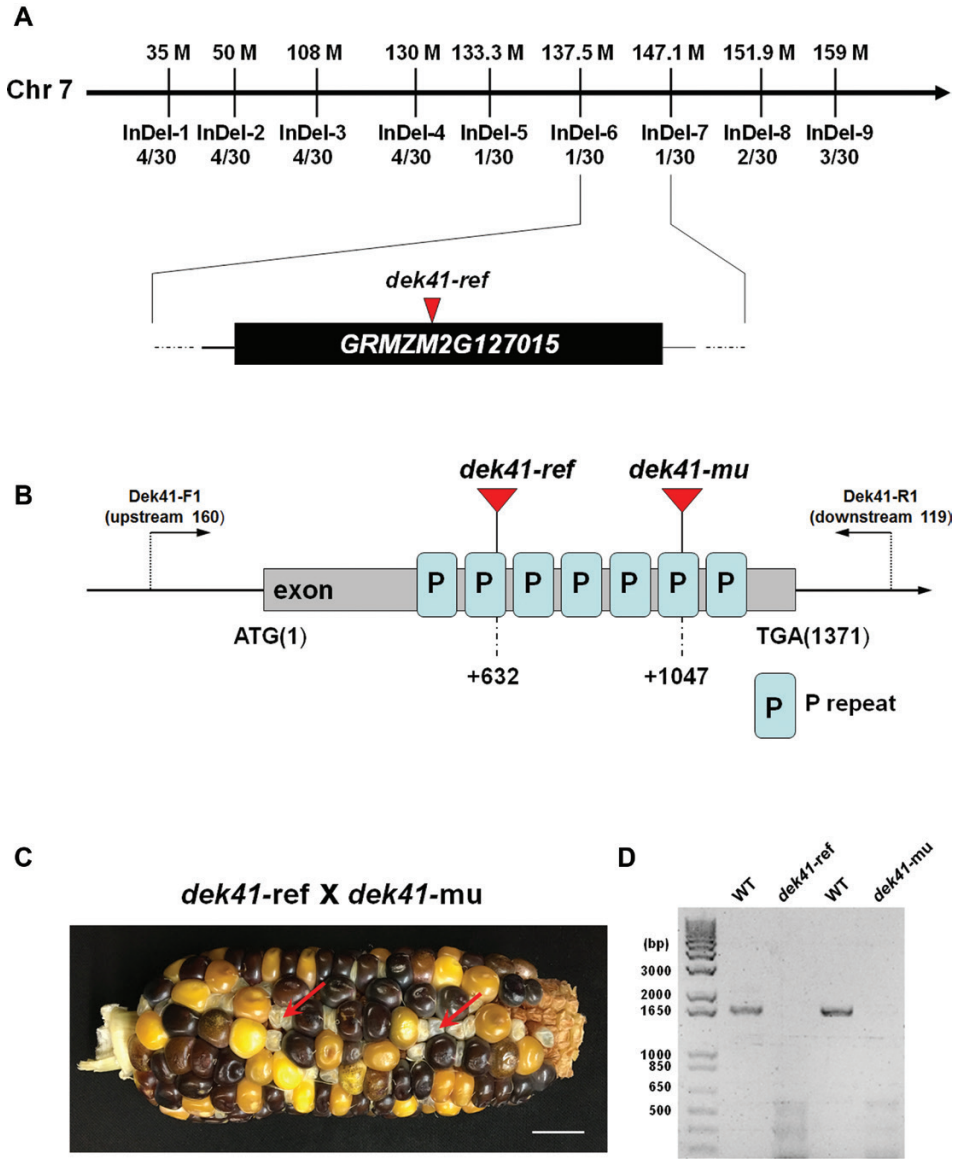

Fig. 2. Cloning and identification of the maize *Dek41* gene. (A) The *Dek41* locus was mapped to an interval of ~9 Mb between molecular markers InDel-6 and InDel-7 on chromosome 7. The triangle indicates the site of *Mu* insertion in the *dek41*-ref mutant. (B) Schematic structure of *GRMZM2G127015* and the allelic mutant. The triangles indicate the sites of *Mu* insertions. The matching positions of the primer pair Dek41-F1/Dek41-R1 that was used for detecting the full-length *Dek41* transcript are indicated. (C) The *dek41*-ref and *dek41*-mu lines were used in allelic tests. The arrows indicate random examples of *dek* (*dek41*-ref/ *dek41*-mu) seeds. (D) Detection of the full-length transcript of *Dek41* in wild-type (WT) and *dek41*-ref seeds at 12 d after pollination by reverse-transcription PCR using the primer pair Dek41-F1/R1, which was mapped to the 5′- and 3′-UTR sequences of *Dek41* mRNA. 18S rRNA was used as the internal control. (This figure is available in colour at *JXB* online.)

was found in the mapped interval, which was located 632 bp downstream of the start codon of *GRMZM2G127015* (Fig. 2B). Thus, *GRMZM2G127015* was the candidate gene for *dek41*.

In addition, a *UniformMu* insertion line (UFMu01110), carrying a *Mu* insertion at 1047 bp downstream of the start codon in *GRMZM2G127015*, was obtained from Maize Genetic Stock Center and named *dek41*-mu in this study (Fig. 2B). To determine whether the mutation in *GRMZM2G127015* was indeed the cause of *dek41*, an allelic test was performed with the mutant allele *dek41*-mu. The test yielded the predicted 3:1 segregation ratio of WT to *dek* seed phenotypes (188:66 for *dek41*-ref × *dek41*-mu and 165:55 for *dek41*-mu × *dek41*-ref, $P<0.05$) (Fig. 2C). Twenty randomly selected seeds (WT and *dek*, 10 for each) from a test-cross ear (*dek41*-ref × *dek41*-mu) were analysed to detect the *Mu* insertion sites by co-segregation (Supplementary Fig. S3). Using the 1s and *Mutir* primers, three types of fragments (394 bps, 809 bps, and no fragment; Supplementary Fig. S3D) were amplified from WT seeds and identical bands (two bands per seed, 394 bps and 809 bps) were amplified from *dek* seeds. Using 1a and *Mutir* primers, three types of fragments (342 bps, 757 bps and no fragment; Supplementary Fig. S3E) were amplified from WT seeds and identical bands (two bands per seed, 757 bps and 342 bps) were amplified from the *dek* seeds. Both the phenotypes of ears in the allelic test and the detection of *Mu* insertion sites by co-segregation confirmed that *dek41-mu* was allelic to *dek41*-ref. Therefore, it was concluded that *GRMZM2G127015* was the causal gene for *dek41*.

Dek41 *encodes a P-type PPR protein*

Sequence analysis of *Dek41* revealed that it consisted of a single exon (without any introns) with a 1371-bp coding sequence encoding a putative PPR protein of 456 amino acids (Fig. 2B). Based on annotation in FLAGdb (http://tools.ips2.u-psud.fr/projects/FLAGdb++/HTML/index.shtml), DEK41 was classified as a P-type PPR protein with seven P repeat domains (Fig. 2B).

Phylogenetic analysis was conducted based on the full-length maize DEK41 protein sequence and homologous protein sequences from other organisms. The results showed that DEK41 homologs were highly conserved in angiosperms (Supplementary Fig. S4A). DEK41 was closely related to Sb02g029280 from *Sorghum bicolor*, to Os05g11700 from *Oryza sativa japonica*, and to homologs from *Setaria italica* (XP_004960609) and *Brachypodium distachyon* (XP_003566429). A detailed sequence alignment with homologs from these species indicated that DEK41 shared highly conserved P repeat domains with homologs in other monocotyledons (Supplementary Fig. S4B).

Dek41 *is constitutively expressed in various tissues*

To examine *Dek41* expression, quantitative RT-PCR was performed using total RNA extracted from immature kernels of the WT and *dek41* mutants at 12, , 15, and 18 DAP. *Ubiquitin* was used as an internal control. Surprisingly, increased transcript levels were detected at 12 DAP and 18 DAP in *dek41* mutants relative to the WT (Supplementary Fig. S5). Full-length *Dek41* transcripts from WT and *dek41* seeds were also detected by reverse-transcription PCR using specific primers Dek41-F1/R1, matching the 5′- and 3′-UTR regional sequences of *Dek41*, respectively (Supplementary Table S2). Full-length (1650-bp) *Dek41* transcripts were detected in WT seeds, but no target bands were amplified from either of the *dek41* mutants (Fig. 2D). These results indicated that the expression of full-length *Dek41* was completely arrested in the *dek41* mutants.

The expression pattern of *Dek41* in the WT was examined by quantitative RT-PCR. It was constitutively expressed in all tested tissues, with the highest expression level being observed in the ear (Fig. 3A). *Dek41* was expressed throughout seed development, from 3–30 DAP, with the highest level recorded at 30 DAP.

DEK41 is targeted to the mitochondria

PPR proteins are predominantly targeted to plastids or mitochondria (Colcombet *et al.*, 2013). To determine the subcellular localization, full-length DEK41 was fused to EYFP in the

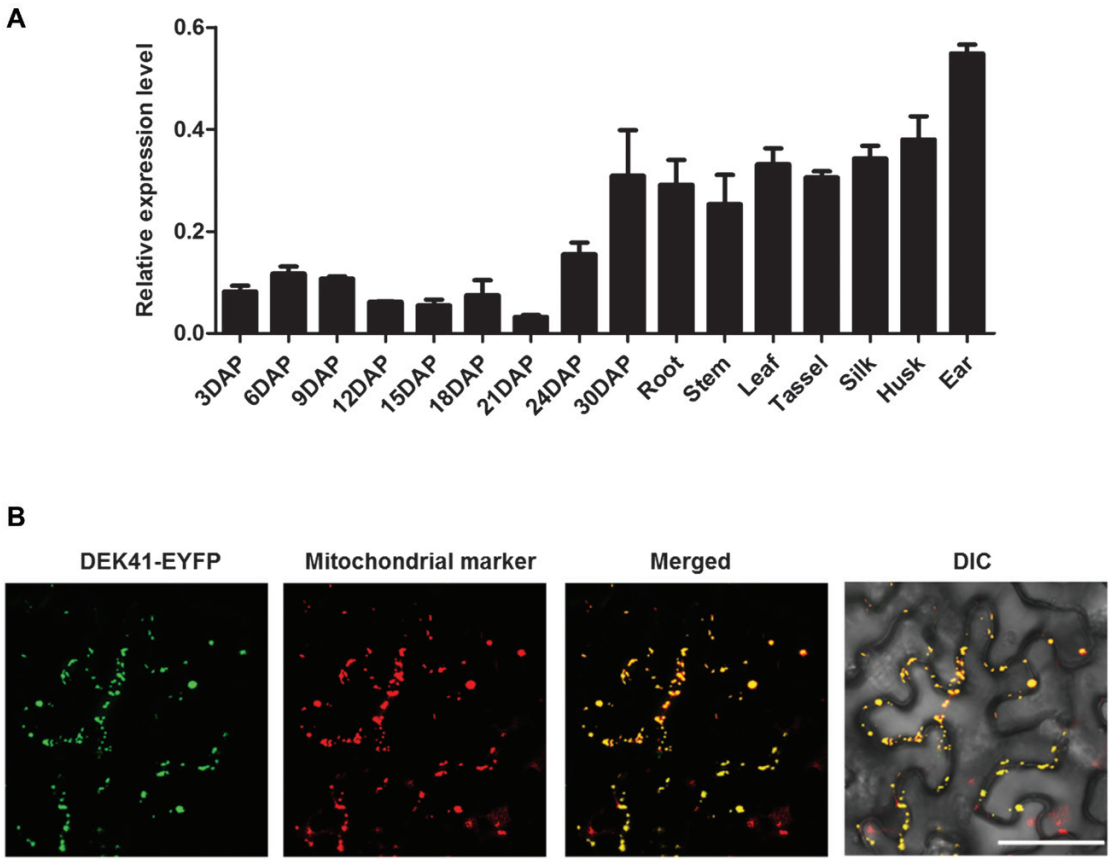

Fig. 3. Expression pattern of maize *Dek41* and subcellular localization of DEK41. (A) RNA expression levels of *Dek41* during seed development and in various tissues. DAP, days after pollination. The tissue samples were taken at the 12-leaf stage. The *Ubiquitin* gene was used as internal control. Data are means (±SE) from *n*=3 plants. Three technical replicates were performed for each RNA sample. (B) Subcellular localization in tobacco leaf epidermal cells. DEK41-EYFP represents the EYFP fusion protein at the C-terminus of the full-length DEK41 protein. The mitochondrial signals are marked by mCherry. DIC, differential interference contrast. Scale bar is 20 μm. (This figure is available in colour at *JXB* online.)

binary vector pB7WGY2.The fusion was transiently expressed in tobacco leaf epidermal cells by *Agrobacterium*-mediated transformation. Confocal laser-scanning microscopy revealed that the EYFP signals co-localized with the mitochondria-mCherry marker pBIN20-MT-RK (Nelson *et al.*, 2007), indicating that DEK41 is targeted to mitochondria (Fig. 3B).

The dek41 *mutation affects* cis*-splicing of mitochondrial* nad4 *intron 3*

As DEK41 is a mitochondria-targeting P-type PPR protein, the transcripts of all the mitochondrial protein-coding genes from immature seeds of the WT and *dek41* mutants at

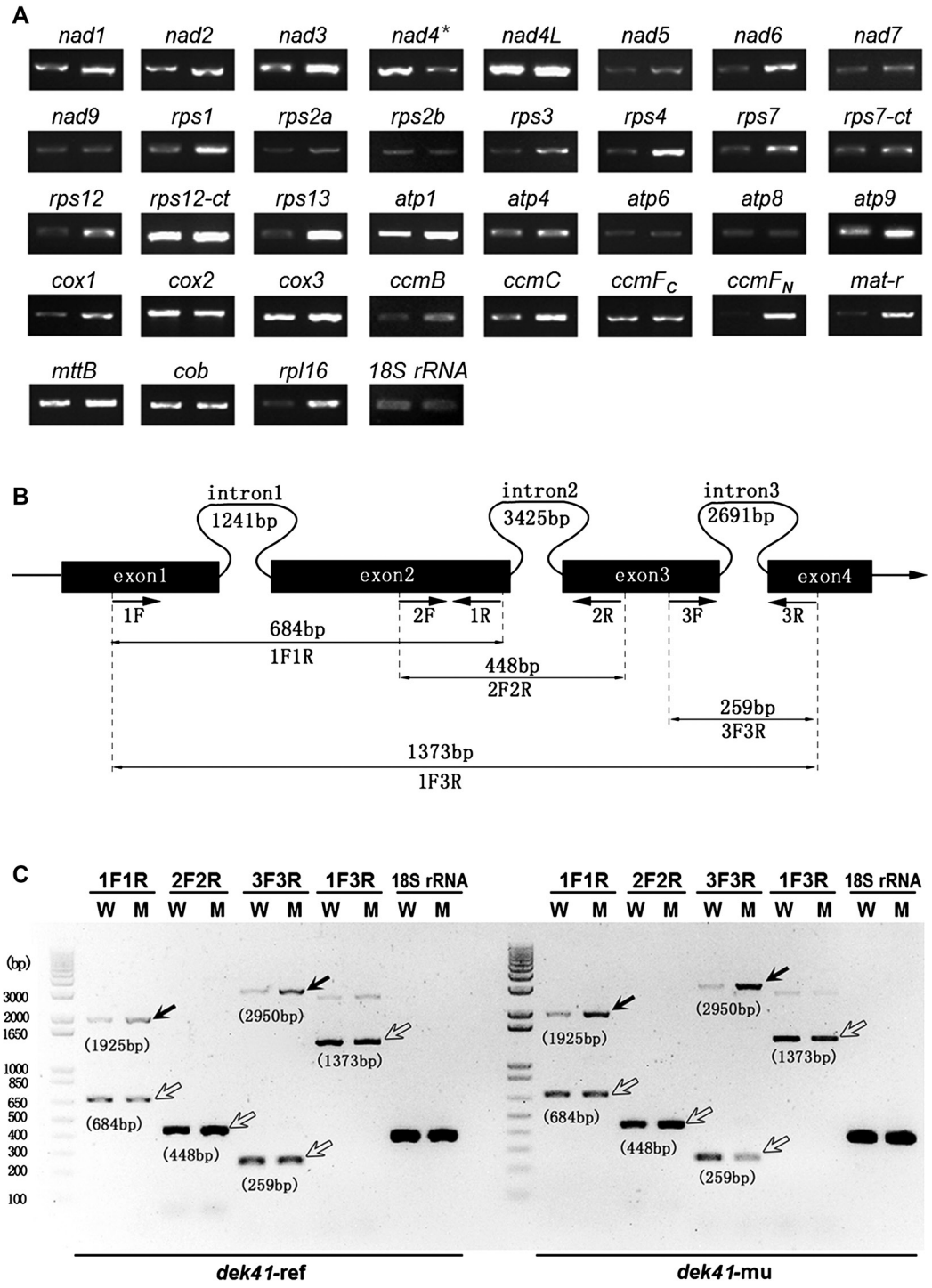

Fig. 4. Decrease of *nad4* mature transcripts and splicing deficiency of *nad4* intron 3 in the maize *dek41* mutants. (A) RT-PCR analysis of 35 mitochondria-encoded transcripts in seeds of the wild-type (WT; left) and *dek41* (right). The RNA was isolated from the same ear segregating for WT and *dek41* seeds at 12 d after pollination. 18S rRNA served as the internal control. The asterisk indicates that *nad4* had decreased transcript abundance. (B) Structure of the maize mitochondrial *nad4* gene. All introns are *cis*-spliced. The expected amplification products using different primer pairs are indicated. (C) RT-PCR analysis of *nad4* intron-splicing efficiency in the WT and *dek41*. Solid arrows indicate unspliced fragments and open arrows indicate spliced fragments. The expected sizes of the amplification products using different primer pairs are indicated below each band. W, wild-type; M, mutant.

12 DAP were amplified by RT-PCR using specific primers (Supplementary Table S2). Among the 35 genes, only the level of mature *nad4* transcript was reduced in *dek41*, whilst the levels of several other genes were increased (Fig. 4A, Supplementary Fig. S6). These results suggested that DEK41 was involved in regulating the expression of *nad4* in developing maize kernels. To further examine the *nad4* precursor transcript, three specific primers were designed to amplify fragments containing each of the three introns in the *nad4* transcript in both *dek41*-ref and *dek41*-mu (Fig. 4B). The splicing efficiencies of *nad4* intron 3 and intron 1 were reduced in *dek41*-ref and *dek41*-mu compared with the WT, whereas the splicing efficiency of *nad4* intron 2 was not affected (Fig. 4C).

P-type PPR proteins are involved in the splicing of group II introns (Cheng *et al.*, 2016; Xiu *et al.*, 2016). Maize mitochondria contain 22 group II introns, including three introns from *nad4* transcripts. To investigate the alterations in splicing in the *dek41* mutants, specific primers were designed for qRT-PCR to inspect all the group II introns in both *dek41*-ref and *dek41*-mu. The quantitative differences in spliced exons between the *dek41* mutants and the WT were compared by PCR using primers across adjacent exons. The results showed a distinct reduction of the *nad4* spliced exon 3–4 fragment and of the splicing efficiency of *nad4* intron 3 in both the mutants compared to the WT (Fig. 5A, B). A slight reduction in splicing efficiency of *nad4* intron 1 was also observed in both the mutants. These results suggested that DEK41 is required for the *cis*-splicing of mitochondrial *nad4* intron 3.

Mutations in Dek41 *affect mitochondrial complex I assembly and NADH dehydrogenase activity*

NAD4 is a subunit of the mitochondrial complex I, NADH dehydrogenase. Blue native polyacrylamide gel electrophoresis (BN-PAGE) was used to detect the potential impact on mitochondrial complexes in *dek41* mutants. The mitochondria were isolated and enriched from immature WT and *dek41* seeds at 18 DAP, and then equivalent amounts of mitochondrial proteins were separated by BN-PAGE. The levels of complex I, as well as super complex I+III$_2$, were reduced in both *dek41*-ref and

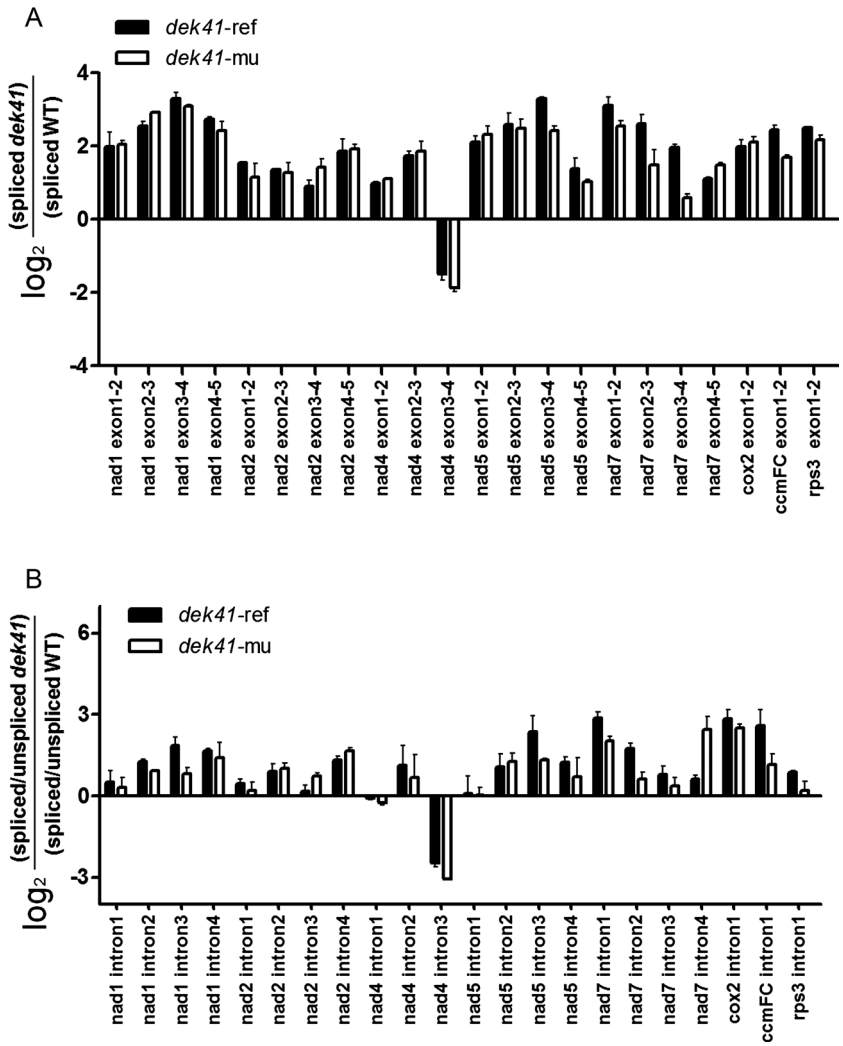

Fig. 5. The maize *dek41* mutation affects *cis*-splicing of mitochondrial *nad4* intron 3. (A) Quantitative RT-PCR analysis of mature transcripts. Primers spanning adjacent exons were used for measuring differences in each spliced fragment. (B) Quantitative RT-PCR analysis of splicing efficiency of mitochondrial introns. The ratio of mature transcripts to unspliced fragments was used to measure differences in splicing efficiency. The *Ubiquitin* gene was used as an internal control. Data are means (±SE) of *n*=3 biological replicates.

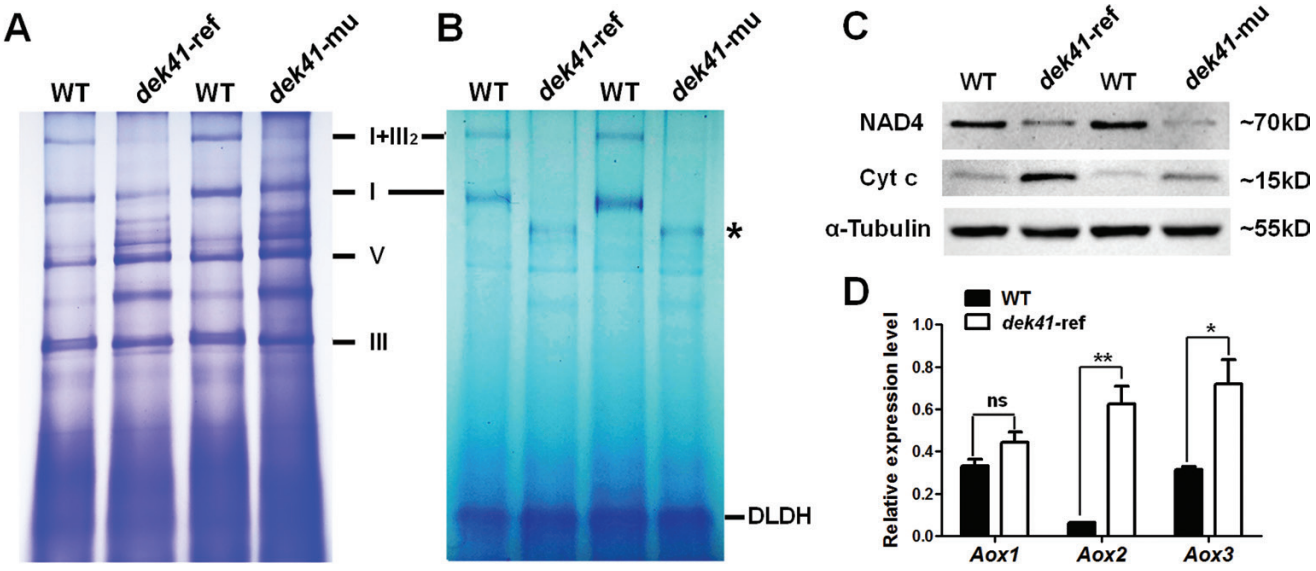

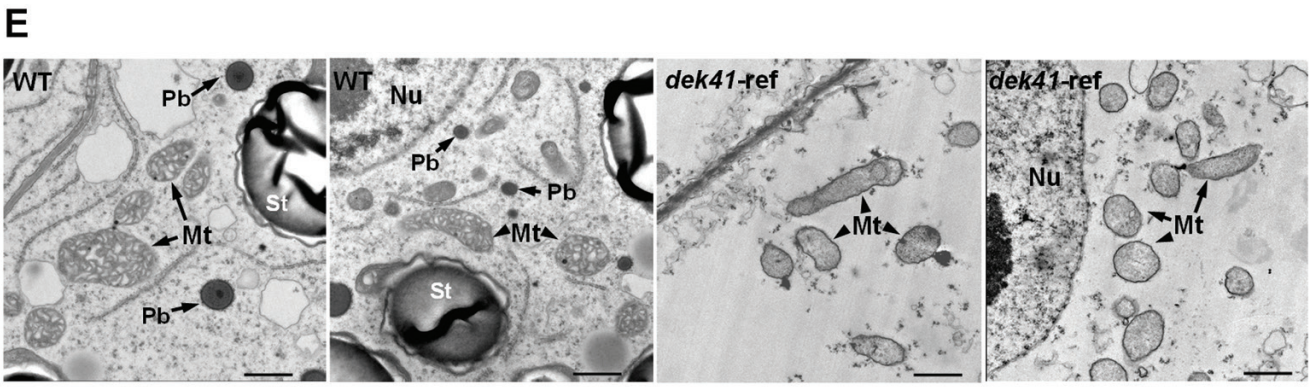

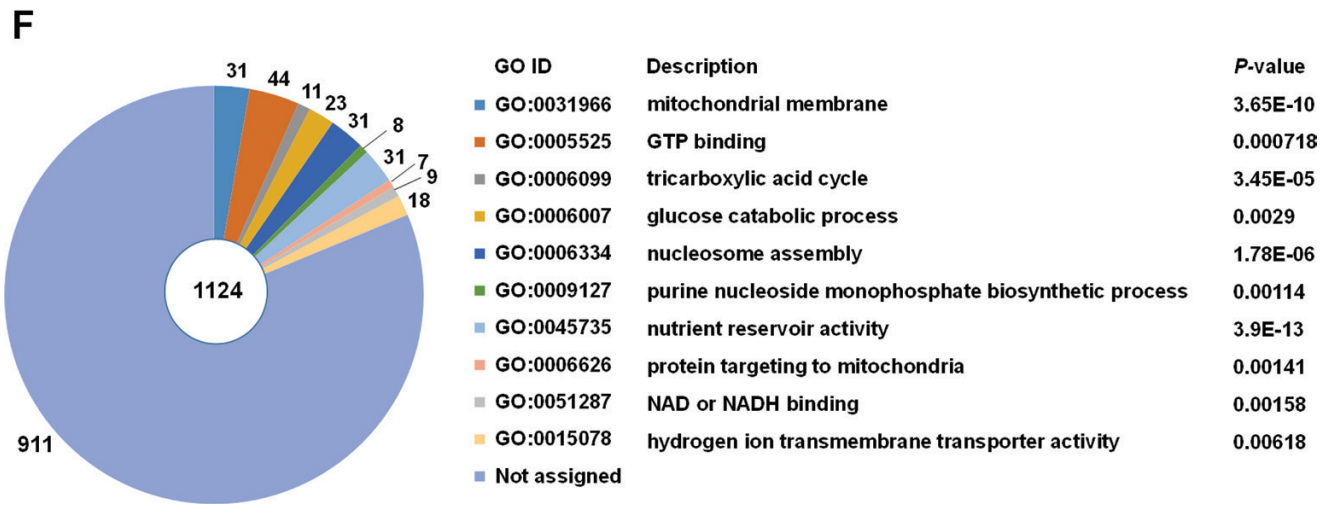

Fig. 6. The maize *dek41* mutation affects mitochondrial functioning in seeds. (A) BN-PAGE analysis of mitochondrial complexes. The positions of complex I, complex III, complex V, and super complex I+III$_2$ (composed of complex I and dimeric complex III) are indicated. Each lane was loaded with 250 μg of mitochondrial protein. WT, wild-type. (B) In-gel NADH dehydrogenase activity test of complex I. The positions of complex I and super complex I+III$_2$ are indicated. * Partially assembled complex I. The activity of dihydrolipoamide dehydrogenase (DLDH) was used as a sample loading control. Each lane was loaded with 250 μg of mitochondrial protein. (C) Western blot comparing accumulation of complex-related protein NAD4 (subunit of complex I) and cytochrome c (Cyt c) in total seed protein from immature WT and *dek41* seeds at 18 d after pollination (DAP). α-Tubulin was used as a sample loading control. (D) Quantitative RT-PCR analysis of *Aox1*, *Aox2*, and *Aox3* that are associated with the alternative respiratory pathway. The *Ubiquitin* gene served as an internal control. Data are means (±SE) of n=3 individuals. Significant differences were determined using Student's t-test: ns, not significant; *P <0.05, **P<0.01. (E) Ultrastructure of developing endosperms from WT and *dek41*-ref seeds at 15 DAP. Scale bars are 1 μm. Nu, nucleus; Mt, mitochondrion; Pb, protein body; St, starch grain. (F) The most significantly enriched GO terms of the 1124 functional annotated differentially expressed genes.

dek41-mu, compared to the WT (Fig. 6A). An in-gel NADH dehydrogenase activity test was conducted to examine the activity of complex I (Meyer *et al.*, 2009). The *dek41* mutants showed significantly reduced complex I and super complex I+III_2 NADH dehydrogenase activity, indicating that the assembly of these complexes was impaired in the mutants (Fig. 6B). A smaller complex I with reduced activity was detected in the mutants, suggesting that a partially assembled complex I maintained residual NADH dehydrogenase activity.

To determine the influence of the *dek41* mutation on oxidation respiratory chain complexes, the levels of mitochondrial complex-related proteins in *dek41* and WT plants were analysed by western blotting using antibodies against NAD4 (subunit of complex I) and cytochrome c. The NAD4 protein was less abundant in the *dek41* mutants, while the amount of cytochrome c was increased (Fig. 6C). The defect of NAD4 was in accordance with the changes observed using BN-PAGE. These results suggested that *dek41* affected the abundance of NAD4 and the assembly of complex I, which probably also affected the accumulation of other proteins related to the electron transport chain (such as cytochrome c) in *dek41*.

dek41 *mutants exhibit abnormal mitochondrial morphology*

To determine the effects of the *dek41* mutation on mitochondrial structure, the endosperms of the WT and *dek41* mutants at 15 DAP were observed by TEM. Normal activation of the electron transport chain (ETC) is required for the proper formation of the inner envelope cristae in mitochondria (Logan, 2006). The mitochondria in the WT endosperm formed distinct inner-envelope cristae surrounded by a dense matrix (Fig. 6E). By contrast, the internal structure of mitochondria in the *dek41* mutants was less distinct, without typical cristae and instead having a grainy appearance. Thus, morphological changes to the mitochondria occurred in *dek41*, suggesting that mitochondrial functioning was severely arrested in the *dek41* during seed development.

The dek41 *mutation affects the expression of genes related to mitochondrial function*

In plants, when there is an electron transport defect in the cytochrome c pathway alternative oxidases (AOXs) are activated to maintain the tricarboxylic acid cycle and electron transport (Vanlerberghe and Ordog, 2002). The alternative pathway was examined by analysing the expression levels of AOX genes in *dek41*. Quantitative RT-PCR showed that both *Aox2* and *Aox3* were up-regulated in *dek41* compared to the WT (Fig. 6D), indicating that the expression levels of genes in the alternative respiratory pathway were up-regulated as the result of inefficient mitochondrial oxidative phosphorylation in the mutant.

The transcript profiles of the endosperm of *dek41* mutants and the WT at 12 DAP were compared using RNA-seq. Among the 41 406 gene transcripts detected, significant DEGs were identified as those with a threshold fold-change >2 and $P<0.001$. Based on these criteria, 1823 genes showed significant altered expression between *dek41* and the WT. There were 1542 genes with increased transcription, while 281 genes showed decreased transcription (Supplementary Table S1). Of these DEGs, 1124 genes could be functionally annotated (BLAST analysis against the GenBank database). Gene ontology (GO; http://bioinfo.cau.edu.cn/agriGO) analysis indicated that the DEGs were mostly related to 10 terms. Among them, six GO terms were closely related to mitochondrial function: 'mitochondrial membrane', 'protein targeting to mitochondria', 'GTP binding', 'NAD or NADH binding', 'purine nucleoside monophosphate biosynthetic process', and 'hydrogen ion transmembrane transporter activity' (Fig. 6F). In addition, DEGs involved in 'tricarboxylic acid cycle', 'glucose catabolic process', and 'nucleosome assembly' were also up-regulated in *dek41*. 'Nutrient reservoir activity', which is mainly attributed to storage proteins, was down-regulated in *dek41* compared with the WT (Supplementary Table S1). This finding was in accordance with the reduced total protein content in mature *dek41* seeds compared to the WT (Supplementary Fig. S2D). The RNA-seq data were further validated by quantitative RT-PCR of some of the most significant DEGs from each GO category (Supplementary Fig. S7), and four basal endosperm transfer layer (BETL) marker genes (BAP-1A, BAP-1B, BETL3, and BETL9) were also detected using qPCR (Supplementary Fig. S8). These results were all in accordance with the RNA-seq data.

Discussion

DEK41 is a P-type PPR protein required for cis*-splicing of mitochondrial* nad4 *intron 3 in maize*

In this study, we identified a novel P-type PPR protein DEK41 that affects the *cis*-splicing of *nad4* intron 3 in maize. Our characterization of DEK41 adds the list of P-type PPR proteins that function as splicing factors in organelle RNA metabolism. P-type PPR proteins with splicing effects have been studied in Arabidopsis mitochondria, and include OTP43, ABO5, OTP439, TANG2, SLO3, and MTL1 (Table 1). These PPRs are required for the splicing of mitochondrial *nad1*, *nad2*, *nad5*, and *nad7* introns. In addition to PPRs, Arabidopsis mutants that affect complex I also include RNA maturase (nMAT1, nMAT2, nMAT4) mutants (Keren *et al.*, 2009, 2012; Cohen *et al.*, 2014) and RNA helicase (PMH2 and ABO6) mutants (He *et al.*, 2012; Köhler *et al.*, 2010). Mutation of these genes (both PPR and non-PPR) in Arabidopsis usually causes a slow-growth phenotype of plants. In maize, the mutants affecting complex I are mostly PPR mutants. The P-type PPRs (EMP8, EMP10, EMP11, EMP16, DEK2, DEK35, and DEK37) are reported to affect the splicing of mitochondrial *nad1*, *nad2*, and *nad4* introns (Table 1). These P-type PPRs together with the PLS-types (Smk1, EMP5, EMP7), which are required for the transcript editing of mitochondrial *nad7*, *rpl16*, and *ccm*F_N (Table 1), affect the assembly of mitochondrial complex I and the corresponding mutants all demonstrate abnormal morphology of mitochondria. The maize *dek10* mutant affects complex IV, the *Emp9* mutant affects complex I and III, and the corresponding genes of these mutants both encode mitochondrial E-subgroup

Table 1. *List of mitochondrial PPR proteins affecting mitochondrial genes in Arabidopsis and maize that are involved in transcript splicing, editing, maturation, stability, and translation*

Function	Organism	Target transcript	Protein	Reference
Splicing	Arabidopsis	*nad1*	OTP43	de Longevialle *et al.* (2007)
Splicing	Arabidopsis	*nad2*	ABO5	Liu *et al.* (2010)
Splicing	Arabidopsis	*nad5*	OTP439	Colas des Francs-Small *et al.* (2014)
Splicing	Arabidopsis	*nad5*	TANG2	Colas des Francs-Small *et al.* (2014)
Splicing	Arabidopsis	*nad7*	SLO3	Hsieh *et al.* (2015)
Splicing	Maize	*nad2*	EMP16	Xiu *et al.* (2016)
Splicing	Maize	*nad2*	EMP10	Cai *et al.* (2017)
Splicing	Maize	*nad4*	DEK35	Chen *et al.* (2017)
Splicing	Maize	*nad1*	DEK2	Qi *et al.* (2017b)
Splicing	Maize	*nad1*	EMP11	Ren *et al.* (2017)
Splicing	Maize	*nad2*	DEK37	Dai *et al.* (2018)
Splicing	Maize	*nad1, nad2, nad4*	EMP8	Sun *et al.* (2018)
Splicing	Maize	*nad4*	DEK41	This study
Editing	Maize	*rpl16, nad9, cox3, rps12*	EMP5	Liu *et al.* (2013)
Editing	Maize	*nad7*	SMK1	Li *et al.* (2014)
Editing	Maize	$ccmF_N$	EMP7	Sun *et al.* (2015)
Maturation	Arabidopsis	*nad9, cox3*	RPF2	Jonietz *et al.* (2010)
Maturation	Arabidopsis	*nad4*	RPF1	Hölzle *et al.* (2011)
Maturation	Arabidopsis	*nad6, atp9*	RPF5	Hauler *et al.* (2013)
Stability	Arabidopsis	*nad4*	MTSF1	Haïli *et al.* (2013)
Stability	Maize	*nad5*	PPR78	Zhang *et al.* (2017)
Translation and splicing	Arabidopsis	*nad7*	MTL1	Haïli *et al.* (2016)

PPRs (Qi *et al.*, 2017a; Yang *et al.*, 2017). The mutants that affect complex I, III, and IV all demonstrate abnormal morphology of mitochondria, indicating that the mitochondrial structure and function are affected. In maize, mutation of these genes usually causes a lethal phenotype of plants (Liu *et al.*, 2013; Qi *et al.*, 2017b; Yang *et al.*, 2017; Dai *et al.*, 2018; Sun *et al.*, 2018).

The maize *dek41*-ref is a defective kernel mutant with arrested endosperm and embryo development (Fig. 1A, D). The full-length *Dek41* transcript was completely repressed in the *dek41*-ref mutant (Fig. 2D), indicating that loss-of-function of DEK41 was the intrinsic cause of the arrested development in *dek41* seed. The splicing efficiency of *nad4* intron 3 was clearly reduced in both the *dek41*-ref and *dek41*-mu mutants, and this was unique across the 22 mitochondrial group II introns (Fig. 5B). Although splicing of *nad4* intron 3 was not completely abolished in the *dek41* mutants, the level of mature *nad4* transcript was reduced (Fig. 4A), which was probably due to a loss of stabilization resulting from a splicing defect. We also noticed that the transcripts of several genes were found to be increased in the *dek41* mutants (such as *nad6*, *rps4*, *rps13*, *atp9*, $ccmF_N$, *matr*, and *rpl16*; Fig. 4A). This could have been due to a feedback response to the mutation in *Dek41*. Similar feedback responses in the transcription of mitochondrial genes have also been observed in other P-type PPR gene mutations (Xiu *et al.*, 2016; Qi *et al.*, 2017b). A slight reduction in splicing efficiency of *nad4* intron 1 was also observed in both the *dek41* mutants (Figs 4C, 5B). However, a reduction in the levels of spliced *nad4* exon1-2 was not found (Fig. 5A), suggesting that *nad4* intron 1 might not be the unique splicing target of DEK41. Our previous work showed that DEK35 also affects the splicing of *nad4* intron 1 (Chen *et al.* 2017), and that EMP8 affects the splicing of mitochondrial *nad4* intron 1, *nad2* intron 1, and *nad1* intron 4 (Sun *et al.*, 2018), so it is possible that the splicing of *nad4* intron 1 requires DEK41, DEK35, and EMP8. Further analysis of mitochondrial complexes showed significant deficiencies of complex I and super complex I + III_2 (Fig. 6A), suggesting that mitochondrial function was severely defective in *dek41* mutants due to reduced *nad4* transcript levels.

NAD4 is one of nine mitochondria-encoded subunits (NAD1–7, NAD4L, and NAD9) that constitute NADH dehydrogenase (Clifton *et al.*, 2004). NADH dehydrogenase is the major entry point for transporting electrons in plants (Braun *et al.*, 2014). Previous studies have shown that different types of nuclear-encoded proteins are involved in the diverse RNA processing of *nad4* transcripts: MTSF1 is essential for the 3′-processing of mitochondrial *nad4* mRNA and its stability in Arabidopsis (Haïli *et al.*, 2013), RPF1 is required for the efficient generation of a 5′-end 228 nucleotides upstream of the mitochondrial *nad4* gene in Arabidopsis (Hölzle *et al.*, 2011), AHG11 has potential roles in *nad4* RNA editing of mitochondria in Arabidopsis (Murayama *et al.*, 2012), CSS1 is a splicing factor of the mitochondrial *nad4* intron in Arabidopsis (Nakagawa and Sakurai, 2006), EMP8 is required for the splicing of mitochondrial *nad4* intron 1 in maize (Sun *et al.*, 2018), and MS1 is involved in splicing of mitochondrial *nad4* intron 1 in *Nicotiana sylvestris* (Brangeon *et al.*, 2000). These studies all report severe effects of faulty regulation of *nad4* transcripts, indicating that NAD4 plays a crucial role in mitochondrial function. In the *dek41* mutants, *nad4* intron 3 exhibited reduced splicing processes, which resulted in severe deficiencies of mitochondrial complex I assembly and activity, and in impaired seed development. Our results demonstrate that splicing of the *nad4* transcript is another crucial post-transcriptional process that is required to maintain the normal function of mitochondrial complex I.

The dek41 *mutation results in defective mitochondrial function and kernel development*

Mitochondrial complex I is the primary entry point for electrons into the electron transport chain (ETC), disruption of which by inhibitors or by loss of subunits leads to problems with primary metabolism (Noctor *et al.*, 2007). Complex I is embedded in the inner membrane and mediates the transfer of electrons from NADH to ubiquinone (Lee *et al.*, 2013). BN-PAGE and in-gel NADH dehydrogenase activity analyses indicated that the assembly and activity of complex I and super-complex I + III_2 were severely impaired in the *dek41* mutants (Fig. 6A, B). A smaller complex I with partial activity was observed in the in-gel NADH dehydrogenase activity assays (Fig. 6B), suggesting that *dek41* mutants can still synthesize proteins in mitochondria, probably at reduced capability and/or with increased errors. Such partially assembled complex Is have also been observed in other PPR mutants, including *emp9*, *ppr78*, and *dek35*, which exhibit arrested mitochondrial complex I activity and seed development (Chen *et al.*, 2017; Yang *et al.*, 2017; Zhang *et al.*, 2017). Similar to *EMP16* (Xiu *et al.*, 2016) and *Dek2* (Qi *et al.*, 2017b), increased *Aox2* and *Aox3* level was also observed in *dek41*. AOXs can reduce the levels of reactive oxygen species in situations when ETC complexes are unable to function properly for the maintenance of electron flux. A rapid increase in transcriptional level of *Aox*s has previously been reported in PPR mutants (Sun *et al.*, 2015; Xiu *et al.*, 2016; Chen *et al.*, 2017; Qi *et al.*, 2017b). Cytochrome c is located in the mitochondrial intermembrane/intercristae spaces and functions as an electron shuttle in the respiratory chain and interacts with cardiolipin (Garrido *et al.*, 2006). Therefore, in addition to the reduction of NAD4 and the increase of cytochrome c in the *dek41* mutants (Fig. 6C), we suggest that the *dek41* mutation affects the assembly and NADH dehydrogenase activity of mitochondrial complex I, which probably promotes the accumulation of other complex-related proteins (including cytochrome c).

ETC biogenesis is required for the proper morphology of the cristae in mitochondria (Logan, 2006). In maize PPR mutants, the formation of mitochondrial cristae by the inner membrane is strongly impaired, and these structurally altered mitochondria are likely less functional than those with a normal inner structure (Sosso *et al.*, 2012; Chen *et al.*, 2017; Qi *et al.*, 2017b; Dai *et al.*, 2018). A voided internal structure with abnormal morphology of mitochondria was also observed in the *dek41* mutants (Fig. 6E), suggesting that mitochondrial function was severely disordered. The loss of DEK41 function results in a defect of ETC biogenesis, which affects not only respiratory metabolism but also the inner structure of the mitochondria.

The defect in mitochondrial function in *dek41* also led to changes in the expression levels of several important genes in GO categories associated with energy-consuming biological process (Fig. 6F). Among 10 GO classifications that were identified as being significantly affected, six that were highly related to mitochondrial structure and activity exhibited extensive up-regulated DEGs, which indicated that the oxidation respiratory chain was severely affected in the *dek41* mutants. The critical effects on mitochondrial function were in accordance with increases identified by transcriptome analysis in 'mitochondrial membrane', 'protein targeting to mitochondria', 'GTP binding', 'NAD or NADH binding', 'hydrogen ion transmembrane transporter activity' and 'purine nucleoside monophosphate biosynthetic process'. The 'tricarboxylic acid cycle' (TCA cycle) is a series of enzyme-catalysed chemical reactions that form a key part of aerobic respiration in mitochondria, and the 'glucose catabolic process' determines the reaction rate of the TCA cycle. 'Nucleosome assembly' is essential for a variety of biological processes, such as cell-cycle progression, development, and senescence (Gal *et al.*, 2015), which are also energy-consuming processes. The *dek41* mutation caused abnormal mitochondrial function, which might have resulted in the feedback up-regulation of genes related to nucleosome assembly, leading in turn to developmental delay (Supplementary Table S1). Whilst GO classifications were up-regulated, only one, 'nutrient reservoir activity', showed decreased DEGs (Supplementary Table S1). Immature *dek41* seeds showed delayed embryo and endosperm development (Fig. 1A, D) and mature seeds exhibited significantly decreased dry weight, and starch and total protein contents (Fig. 1G, H, Supplementary Fig. S2D). These phenotypic data were in accordance with the decreased DEGs identified in the transcriptome analysis (Supplementary Table S1). We postulate that the wide down-regulation of genes encoding zein proteins might explain the reduced total protein content in the seeds. Our results highlight the necessity of mitochondrial activity for nutrient generation and accumulation (Law *et al.*, 2014).

The basal endosperm transfer layer (BETL) develops extensive cell-wall ingrowths that support an enlarged plasma membrane surface, promoting primary nutrient uptake in the endosperm (Pate and Gunning, 1972; Thompson *et al.*, 2001; Offler *et al.*, 2003) that requires high metabolic rates. Therefore, transfer cells are typically rich in mitochondria. In our study, the development of the BETL was dramatically arrested in *dek41* (Fig. 1F), and the transcriptional levels of BETL marker genes were decreased (Supplementary Fig. S8). The absence of a properly formed transfer cell layer is always correlated with reduced rates of grain filling and with seed abortion (Brink and Cooper, 1947; Charlton *et al.*, 1995), and mutants with arrested BETL development exhibit small and hollow kernels. Mutations of maize *EMP4*, *EMP16*, *DEK35*, and *DEK37* that encode PPR proteins also result in a defective transfer cell layer (Gutierrez *et al.*, 2007; Xiu *et al.*, 2016; Chen *et al.*, 2017; Dai *et al.*, 2018). Therefore, the arrested development of the BETL in *dek41* might be the consequence of reduced energy for nutrient transport. In summary, the *dek41* mutation in maize affects the mitochondrial structure and function, resulting in arrested BETL formation and embryo morphogenesis, which ultimately affects kernel development.

Supplementary data

Supplementary data are available at *JXB* online.

Fig. S1. Original gels of western blots comparing accumulation of NAD4 in total proteins from immature wild-type and *dek41* seeds at 18 DAP.

Fig. S2. Analysis of protein content in the maize *dek41* mutant.

Fig. S3. Detection of *Mu* insertion sites by co-segregation for test-cross ears of *dek41*-ref × *dek41*-mu.

Fig. S4. Phylogenetic analysis and sequence alignment of DEK41 with its homologs.

Fig. S5. Quantitative RT-PCR comparing *Dek41* transcript levels in the wild-type and *dek41* at 12, 15, and 18 DAP.

Fig. S6. Original gels used for RT-PCR analysis of 35 mitochondria-encoded transcripts in immature wild-type and *dek41* seeds at 12 DAP.

Fig. S7. Quantitative RT-PCR confirmation of the transcriptome data.

Fig. S8. Quantitative RT-PCR identification of BETL marker genes in immature *dek41*-ref and wild-type seeds at 15 DAP and 18 DAP.

Table S1. Gene ontology classifications of DEGs with functional annotations.

Table S2. Primers used in this study.

Acknowledgements

This work was supported by the National Key Research and Development Program of China (2016YFD0101003) and the National Natural Sciences Foundation of China (91635303 and 31425019). The authors thank Yanan Feng and Yihong Yue for their kind assistance in positional cloning of *Dek41*.

References

Barkan A, Small I. 2014. Pentatricopeptide repeat proteins in plants. Annual Review of Plant Biology **65**, 415–442.

Berrisford JM, Sazanov LA. 2009. Structural basis for the mechanism of respiratory complex I. The Journal of Biological Chemistry **284**, 29773–29783.

Bonen L. 2008. *Cis*- and *trans*-splicing of group II introns in plant mitochondria. Mitochondrion **8**, 26–34.

Brangeon J, Sabar M, Gutierres S, *et al.* 2000. Defective splicing of the first *nad4* intron is associated with lack of several complex I subunits in the *Nicotiana sylvestris* NMS1 nuclear mutant. The Plant Journal **21**, 269–280.

Braun HP, Binder S, Brennicke A, *et al.* 2014. The life of plant mitochondrial complex I. Mitochondrion **19**, 295–313.

Brink RA, Cooper DC. 1947. Effect of the De_{17} allele on development of the maize caryopsis. Genetics **32**, 350–368.

Brown GG, Colas des Francs-Small C, Ostersetzer-Biran O. 2014. Group II intron splicing factors in plant mitochondria. Frontiers in Plant Science **5**, 35.

Burger G, Gray MW, Lang BF. 2003. Mitochondrial genomes: anything goes. Trends in Genetics **19**, 709–716.

Cai M, Li S, Sun F, Sun Q, Zhao H, Ren X, Zhao Y, Tan BC, Zhang Z, Qiu F. 2017. *Emp10* encodes a mitochondrial PPR protein that affects the *cis*-splicing of *nad2* intron 1 and seed development in maize. The Plant Journal **91**, 132–144.

Charlton WL, Keen CL, Merriman C, Lynch P, Greenland AJ, Dickinson HG. 1995. Endosperm development in *Zea mays*: implication of gametic imprinting and paternal excess in regulation of transfer layer development. Development **121**, 3089–3097.

Chen X, Feng F, Qi W, Xu L, Yao D, Wang Q, Song R. 2017. *Dek35* encodes a PPR protein that affects *cis*-splicing of mitochondrial *nad4* intron 1 and seed development in maize. Molecular Plant **10**, 427–441.

Cheng S, Gutmann B, Zhong X, *et al.* 2016. Redefining the structural motifs that determine RNA binding and RNA editing by pentatricopeptide repeat proteins in land plants. The Plant Journal **85**, 532–547.

Clayton DA, Shadel GS. 2014. Isolation of mitochondria from cells and tissues. Cold Spring Harbor Protocols **2014**, pdb.top074542.

Clifton SW, Minx P, Fauron CM, *et al.* 2004. Sequence and comparative analysis of the maize NB mitochondrial genome. Plant Physiology **136**, 3486–3503.

Cohen S, Zmudjak M, Colas des Francs-Small C, *et al.* 2014. nMAT4, a maturase factor required for *nad1* pre-mRNA processing and maturation, is essential for holocomplex I biogenesis in *Arabidopsis* mitochondria. The Plant Journal **78**, 253–268.

Colas des Francs-Small C, Falcon de Longevialle A, Li Y, Lowe E, Tanz SK, Smith C, Bevan MW, Small I. 2014. The pentatricopeptide repeat proteins TANG2 and ORGANELLE TRANSCRIPT PROCESSING439 are involved in the splicing of the multipartite *nad5* transcript encoding a subunit of mitochondrial complex I. Plant Physiology **165**, 1409–1416.

Colcombet J, Lopez-Obando M, Heurtevin L, Bernard C, Martin K, Berthomé R, Lurin C. 2013. Systematic study of subcellular localization of *Arabidopsis* PPR proteins confirms a massive targeting to organelles. RNA Biology **10**, 1557–1575.

Dai D, Luan S, Chen X, Wang Q, Feng Y, Zhu C, Qi W, Song R. 2018. Maize *Dek37* encodes a P-type PPR protein that affects *cis*-splicing of mitochondrial *nad2* intron 1 and seed development. Genetics **208**, 1069–1082.

de Longevialle AF, Meyer EH, Andrés C, Taylor NL, Lurin C, Millar AH, Small ID. 2007. The pentatricopeptide repeat gene *OTP43* is required for *trans*-splicing of the mitochondrial *nad1* Intron 1 in *Arabidopsis thaliana*. The Plant Cell **19**, 3256–3265.

Feng L, Zhu J, Wang G, Tang Y, Chen H, Jin W, Wang F, Mei B, Xu Z, Song R. 2009. Expressional profiling study revealed unique expressional patterns and dramatic expressional divergence of maize α-zein super gene family. Plant Molecular Biology **69**, 649–659.

Fujii S, Small I. 2011. The evolution of RNA editing and pentatricopeptide repeat genes. New Phytologist **191**, 37–47.

Gal C, Moore KM, Paszkiewicz K, Kent NA, Whitehall SK. 2015. The impact of the HIRA histone chaperone upon global nucleosome architecture. Cell Cycle **14**, 123–134.

Garrido C, Galluzzi L, Brunet M, Puig PE, Didelot C, Kroemer G. 2006. Mechanisms of cytochrome c release from mitochondria. Cell Death and Differentiation **13**, 1423–1433.

Gorchs Rovira A, Smith AG. 2019. PPR proteins – orchestrators of organelle RNA metabolism. Physiologia Plantarum **166**, 451–459.

Gutierrez L, Van Wuytswinkel O, Castelain M, Bellini C. 2007. Combined networks regulating seed maturation. Trends in Plant Science **12**, 294–300.

Haïli N, Arnal N, Quadrado M, Amiar S, Tcherkez G, Dahan J, Briozzo P, Colas des Francs-Small C, Vrielynck N, Mireau H. 2013. The pentatricopeptide repeat MTSF1 protein stabilizes the *nad4* mRNA in *Arabidopsis* mitochondria. Nucleic Acids Research **41**, 6650–6663.

Haïli N, Planchard N, Arnal N, Quadrado M, Vrielynck N, Dahan J, des Francs-Small CC, Mireau H. 2016. The MTL1 pentatricopeptide repeat protein is required for both translation and splicing of the mitochondrial NADH DEHYDROGENASE SUBUNIT7 mRNA in *Arabidopsis*. Plant Physiology **170**, 354–366.

Hammani K, Giegé P. 2014. RNA metabolism in plant mitochondria. Trends in Plant Science **19**, 380–389.

Hauler A, Jonietz C, Stoll B, Stoll K, Braun HP, Binder S. 2013. RNA PROCESSING FACTOR 5 is required for efficient 5′ cleavage at a processing site conserved in RNAs of three different mitochondrial genes in *Arabidopsis thaliana*. The Plant Journal **74**, 593–604.

He J, Duan Y, Hua D, Fan G, Wang L, Liu Y, Chen Z, Han L, Qu LJ, Gong Z. 2012. DEXH box RNA helicase-mediated mitochondrial reactive oxygen species production in *Arabidopsis* mediates crosstalk between abscisic acid and auxin signaling. The Plant Cell **24**, 1815–1833.

Hölzle A, Jonietz C, Törjek O, Altmann T, Binder S, Forner J. 2011. A RESTORER OF FERTILITY-like PPR gene is required for 5′-end processing of the *nad4* mRNA in mitochondria of *Arabidopsis thaliana*. The Plant Journal **65**, 737–744.

Hsieh WY, Liao JC, Chang CY, Harrison T, Boucher C, Hsieh MH. 2015. The SLOW GROWTH3 pentatricopeptide repeat protein is required for the splicing of mitochondrial *NADH dehydrogenase subunit7* intron 2 in *Arabidopsis*. Plant Physiology **168**, 490–501.

Jonietz C, Forner J, Hölzle A, Thuss S, Binder S. 2010. RNA PROCESSING FACTOR2 is required for 5′ end processing of *nad9* and *cox3* mRNAs in mitochondria of *Arabidopsis thaliana*. The Plant Cell **22**, 443–453.

Keren I, Bezawork-Geleta A, Kolton M, Maayan I, Belausov E, Levy M, Mett A, Gidoni D, Shaya F, Ostersetzer-Biran O. 2009. AtnMat2, a nuclear-encoded maturase required for splicing of group-II introns in *Arabidopsis* mitochondria. RNA **15**, 2299–2311.

Keren I, Tal L, des Francs-Small CC, Araújo WL, Shevtsov S, Shaya F, Fernie AR, Small I, Ostersetzer-Biran O. 2012. *nMAT1*, a nuclear-encoded maturase involved in the *trans*-splicing of *nad1* intron 1, is essential for mitochondrial complex I assembly and function. The Plant Journal **71**, 413–426.

Köhler D, Schmidt-Gattung S, Binder S. 2010. The DEAD-box protein PMH2 is required for efficient group II intron splicing in mitochondria of *Arabidopsis thaliana*. Plant Molecular Biology **72**, 459–467.

Langmead B, Salzberg SL. 2012. Fast gapped-read alignment with Bowtie 2. Nature Methods **9**, 357–359.

Law SR, Narsai R, Whelan J. 2014. Mitochondrial biogenesis in plants during seed germination. Mitochondrion **19**, 214–221.

Lee CP, Taylor NL, Millar AH. 2013. Recent advances in the composition and heterogeneity of the *Arabidopsis* mitochondrial proteome. Frontiers in Plant Science **4**, 4.

Li XJ, Zhang YF, Hou M, *et al.* 2014. *Small kernel 1* encodes a pentatricopeptide repeat protein required for mitochondrial *nad7* transcript editing and seed development in maize (*Zea mays*) and rice (*Oryza sativa*). The Plant Journal **79**, 797–809.

Lid SE, Gruis D, Jung R, Lorentzen JA, Ananiev E, Chamberlin M, Niu X, Meeley R, Nichols S, Olsen OA. 2002. The *defective kernel 1* (*dek1*) gene required for aleurone cell development in the endosperm of maize grains encodes a membrane protein of the calpain gene superfamily. Proceedings of the National Academy of Sciences, USA **99**, 5460–5465.

Liu Y, He J, Chen Z, Ren X, Hong X, Gong Z. 2010. *ABA overly-sensitive 5* (*ABO5*), encoding a pentatricopeptide repeat protein required for *cis*-splicing of mitochondrial *nad2* intron 3, is involved in the abscisic acid response in *Arabidopsis*. The Plant Journal **63**, 749–765.

Liu YJ, Xiu ZH, Meeley R, Tan BC. 2013. *Empty pericarp5* encodes a pentatricopeptide repeat protein that is required for mitochondrial RNA editing and seed development in maize. The Plant Cell **25**, 868–883.

Logan DC. 2006. The mitochondrial compartment. Journal of Experimental Botany **57**, 1225–1243.

Lurin C, Andrés C, Aubourg S, *et al.* 2004. Genome-wide analysis of *Arabidopsis* pentatricopeptide repeat proteins reveals their essential role in organelle biogenesis. The Plant Cell **16**, 2089–2103.

Meyer EH, Tomaz T, Carroll AJ, Estavillo G, Delannoy E, Tanz SK, Small ID, Pogson BJ, Millar AH. 2009. Remodeled respiration in *ndufs4* with low phosphorylation efficiency suppresses *Arabidopsis* germination and growth and alters control of metabolism at night. Plant Physiology **151**, 603–619.

Møller IM. 2016. What is hot in plant mitochondria? Physiologia Plantarum **157**, 256–263.

Mortazavi A, Williams BA, McCue K, Schaeffer L, Wold B. 2008. Mapping and quantifying mammalian transcriptomes by RNA-seq. Nature Methods **5**, 621–628.

Murayama M, Hayashi S, Nishimura N, Ishide M, Kobayashi K, Yagi Y, Asami T, Nakamura T, Shinozaki K, Hirayama T. 2012. Isolation of *Arabidopsis ahg11*, a weak ABA hypersensitive mutant defective in *nad4* RNA editing. Journal of Experimental Botany **63**, 5301–5310.

Nakagawa N, Sakurai N. 2006. A mutation in *At-nMat1a*, which encodes a nuclear gene having high similarity to group II intron maturase, causes impaired splicing of mitochondrial NAD4 transcript and altered carbon metabolism in *Arabidopsis thaliana*. Plant & Cell Physiology **47**, 772–783.

Nelson BK, Cai X, Nebenführ A. 2007. A multicolored set of *in vivo* organelle markers for co-localization studies in *Arabidopsis* and other plants. The Plant Journal **51**, 1126–1136.

Neuffer MG, Sheridan WF. 1980. Defective kernel mutants of maize. I. Genetic and lethality studies. Genetics **95**, 929–944.

Noctor G, De Paepe R, Foyer CH. 2007. Mitochondrial redox biology and homeostasis in plants. Trends in Plant Science **12**, 125–134.

Offler CE, McCurdy DW, Patrick JW, Talbot MJ. 2003. Transfer cells: cells specialized for a special purpose. Annual Review of Plant Biology **54**, 431–454.

Pate JS, Gunning BES. 1972. Transfer cells. Annual Review in Plant Physiology **23**, 173–196.

Qi W, Tian Z, Lu L, Chen X, Chen X, Zhang W, Song R. 2017a. Editing of mitochondrial transcripts *nad3* and *cox2* by Dek10 is essential for mitochondrial function and maize plant development. Genetics **205**, 1489–1501.

Qi W, Yang Y, Feng X, Zhang M, Song R. 2017b. Mitochondrial function and maize kernel development requires Dek2, a pentatricopeptide repeat protein involved in *nad1* mRNA splicing. Genetics **205**, 239–249.

Qi W, Zhu J, Wu Q, Wang Q, Li X, Yao D, Jin Y, Wang G, Wang G, Song R. 2016. Maize *reas1* mutant stimulates ribosome use efficiency and triggers distinct transcriptional and translational responses. Plant Physiology **170**, 971–988.

Ren X, Pan Z, Zhao H, Zhao J, Cai M, Li J, Zhang Z, Qiu F. 2017. EMPTY PERICARP11 serves as a factor for splicing of mitochondrial *nad1* intron and is required to ensure proper seed development in maize. Journal of Experimental Botany **68**, 4571–4581.

Sazanov LA, Hinchliffe P. 2006. Structure of the hydrophilic domain of respiratory complex I from *Thermus thermophilus*. Science **311**, 1430–1436.

Sosso D, Mbelo S, Vernoud V, *et al.* 2012. PPR2263, a DYW-subgroup pentatricopeptide repeat protein, is required for mitochondrial *nad5* and *cob* transcript editing, mitochondrion biogenesis, and maize growth. The Plant Cell **24**, 676–691.

Sun F, Wang X, Bonnard G, Shen Y, Xiu Z, Li X, Gao D, Zhang Z, Tan BC. 2015. *Empty pericarp7* encodes a mitochondrial E-subgroup pentatricopeptide repeat protein that is required for *ccmFN* editing, mitochondrial function and seed development in maize. The Plant Journal **84**, 283–295.

Sun F, Zhang X, Shen Y, Wang H, Liu R, Wang X, Gao D, Yang YZ, Liu Y, Tan BC. 2018. The pentatricopeptide repeat protein EMPTY PERICARP8 is required for the splicing of three mitochondrial introns and seed development in maize. The Plant Journal **95**, 919–932.

Tamura K, Dudley J, Nei M, Kumar S. 2007. MEGA4: molecular evolutionary genetics analysis (MEGA) software version 4.0. Molecular Biology and Evolution **24**, 1596–1599.

Thompson JD, Gibson TJ, Plewniak F, Jeanmougin F, Higgins DG. 1997. The CLUSTAL_X windows interface: flexible strategies for multiple sequence alignment aided by quality analysis tools. Nucleic Acids Research **25**, 4876–4882.

Thompson RD, Hueros G, Becker H, Maitz M. 2001. Development and functions of seed transfer cells. Plant Science **160**, 775–783.

van Herpen TW, Cankar K, Nogueira M, Bosch D, Bouwmeester HJ, Beekwilder J. 2010. *Nicotiana benthamian*a as a production platform for artemisinin precursors. PLoS ONE **5**, e14222.

Vanlerberghe GC, Ordog SH. 2002. Alternative oxidase: integrating carbon metabolism and electron transport in plant respiration. In: Foyer GH, Noctor G, eds. Advances in photosynthesis and respiration, photosynthetic nitrogen assimilation and associated carbon and respiratory metabolism. Dordrect, Netherlands: Kluwer Academic Publishers, 173–191.

Williams-Carrier R, Stiffler N, Belcher S, Kroeger T, Stern DB, Monde RA, Coalter R, Barkan A. 2010. Use of Illumina sequencing to identify transposon insertions underlying mutant phenotypes in high-copy *Mutator* lines of maize. The Plant Journal **63**, 167–177.

Xiu Z, Sun F, Shen Y, Zhang X, Jiang R, Bonnard G, Zhang J, Tan BC. 2016. EMPTY PERICARP16 is required for mitochondrial *nad2* intron 4 *cis*-splicing, complex I assembly and seed development in maize. The Plant Journal **85**, 507–519.

Yang YZ, Ding S, Wang HC, Sun F, Huang WL, Song S, Xu C, Tan BC. 2017. The pentatricopeptide repeat protein EMP9 is required for mitochondrial *ccmB* and *rps4* transcript editing, mitochondrial complex biogenesis and seed development in maize. New Phytologist **214**, 782–795.

Zhang YF, Suzuki M, Sun F, Tan BC. 2017. The mitochondrion-targeted PENTATRICOPEPTIDE REPEAT78 protein is required for *nad5* mature mRNA stability and seed development in maize. Molecular Plant **10**, 1321–1333.